Geophysical Journal International

Geophys. J. Int. (2023) **232,** 1545–1555
Advance Access publication 2022 October 11
GJI Seismology

https://doi.org/10.1093/gji/ggac403

Anomalies and transient variations of *b*-value in Italy during the major earthquake sequences: what truth is there to this?

A.M. Lombardi

Istituto Nazionale di Geofisica e Vulcanologia, Rome 00143*, Italy. E-mail:* annamaria.lombardi@ingv.it

Accepted 2022 October 7. Received 2022 September 13; in original form 2022 July 1

SUMMARY

The Gutenberg–Richter *b*-value is thought to be a proxy of stress conditions in the crust and therefore able to locate asperities as zones of stress concentration responsible for the nucleation of strong events. The scientific literature contains a broad range of case studies showing precursory drops of *b*, just before the occurrence of strong events, and subsequent rises, during the early part of aftershocks sequences. Translating these results into hazard assessment, the *b*-value has assumed the status of a candidate precursor to the occurrence of an imminent large event. This issue is analysed here for three major seismic sequences that occurred recently in Italy. In comparison to previous studies, this investigation indicates that the variability of *b* may not be a reliable indicator of stress or a significant precursor in these examples, and instead may be assigned to a combination of chance, inhomogeneities in the data and inefficiencies in estimation methodologies. Consequently, extreme caution is required when we interpret *b*-values both as a proxy of physical processes involved in a seismic sequence and as a precursor to the occurrence of imminent strong events.

Key words: Statistical methods; Earthquake interaction, forecasting, and prediction; Statistical seismology.

1 INTRODUCTION

The earthquake frequency–magnitude distribution is most commonly described by the 'Gutenberg–Richter Law' (GRL; Ishimoto & Iida 1939; Gutenberg & Richter 1942), which, in mathematical terms, is expressed by the equation

$$\log_{10}[N(M)] = a - b \cdot M, \qquad (1)$$

where *a* (productivity) and *b* (slope) are constants and $N(M)$ is the number of events with magnitude equal to or above *M*. By a strictly statistical point of view, the GRL leads to a continuous exponential or to a discrete geometric (to account for binning of magnitudes) probability distribution for magnitudes (Aki 1965; Bender 1983; Tinti & Mulargia 1987; Marzocchi & Sandri 2003; Lombardi 2021). The estimates of *b* obtained using the continuous or discrete formulae are nearly identical for a binning of 0.1, commonly adopted for instrumental data.

Since the publication of the GRL, up to the present time, a great amount of studies was carried out in this field, concerning both technical and interpretative issues. The evaluation of the parameter *b* is, to this day, one the most frequently performed statistical calculations in seismology and takes an important role in earthquake hazard assessment and in characterizing the tectonic setting of a region. Inspired from numerical modelling (Kun *et al.* 2013) and laboratory experiments (Scholz 1968; Main *et al.* 1989, 1992; Amitrano 2003; Goebel *et al.* 2012), most of these studies have tried to answer the important question of whether significant variations of the *b*-value exist and what is their relationship to the physical properties of the earthquake rupture, such as focal depth, tectonic frameworks or stress evolution (Mogi 1962; Scholz 1968; Wyss 1973; Rundle *et al.* 2000; Wiemer & Wyss 2000; Schorlemmer *et al.* 2005; Gulia & Wiemer 2019).

The supposed physical meaning of *b* suggested that studies on the *b*-value heterogeneity might help in understanding the mechanism of earthquake sequences and enable predictions during a sequence. In several decades, a lot of studies have addressed the problem of the temporal and spatial changes in the *b*-value, before the main-shock occurrence and throughout the following aftershocks sequences (e.g. Smith 1981; Suyehiro 1966; Utsu 1970, 1971; Gibowicz 1973; Wyss & Lee 1973; Wiemer & Wyss 1997; Schorlemmer & Wiemer 2005; Tormann *et al.* 2012; Gulia & Wiemer 2019). The scientific community is far from being unanimous on both methodological and interpretative issue. This dissimilarity of viewpoints is not surprising if one acknowledges all factors that could affect *b*-value calculations: the choice of threshold magnitude, the binning and the measurement errors of magnitudes, the sample size, the width of the range covered by magnitude data, the mixing of magnitude types, the changes in the seismic network detection, the lack of statistical rigor in the analysis (Kagan 1999; Wiemer & Wyss 2000; Marzocchi & Sandri 2003; Amorèse *et al.* 2010; Geffers *et al.* 2022). Therefore, whereas some seismologists present their results to support the heterogeneity of *b*, other studies interpret the *b*-value variability as an artefact due to methodological errors and to chance.

Given the laboratory evidence that the *b*-value is inversely proportional to stress, many studies use that the frequency–magnitude relationship has a stress meter, to visualize highly stressed portions of the crust and for mapping fault asperities (Wiemer & Wyss 1997; Schorlemmer & Wiemer 2005). A number of large earthquakes have been supposed to have ruptured areas of low pre–main-shock *b* values (Tormann *et al.* 2012; Schurr *et al.* 2014; Tormann *et al.* 2015), so that low *b*-values were proposed as a good proxy for sizing the asperities capable of large slip, opening new perspectives to measurement or real-time monitoring of *b*-values for short-term hazard purposes (Wyss & Lee 1973; Wiemer & Katsumata 1999; Schorlemmer & Wiemer 2005; Gulia & Wiemer 2019). On a longer temporal scale, some studies demonstrated that the occurrence of large events may be anticipated by a period of some years of high *b*-values (Fielder 1974; Smith 1981, 1986, 1998; Oncel & Wilson 2007), consistently with some evidence of a decreasing moderate-magnitude seismic activity prior to large earthquakes (Mogi 1979).

The studies more focused on technical aspects and statistical requirements of *b* and M_c estimation instead recommend a cautious interpretation of supposed *b*-value changes. The arguments brought forward for such a position mainly relate to problems in M_c evaluation (Amorèse 2007; Zaliapin & Ben-Zion 2015), critical issues of magnitude data (Zúñiga & Wyss 1995; Main 2000; Marzocchi & Sandri 2003; Kamer & Hiemer 2015; Marzocchi *et al.* 2020; Geffers *et al.* 2022) and procedures used for significance testing (Amorèse *et al.* 2010). Noteworthy, none systematic experiment done for searching significant precursors, as the International Association of Seismology and Physics of the Earth's Interior (IASPEI) exercise (Wyss & Booth 1997) or the Collaboratory for the Study of Earthquake Predictability (CSEP) experiment (https://cseptesting.org/; Jordan 2006), supports the forecasting performance of *b*-value anomalies (Wyss 1997; Taroni *et al.* 2018). Similar cautious conclusions were reached by Jordan *et al.* (2011), in their review on the operational earthquake forecasting.

The estimated values of the *b* parameter and, much more, of the completeness magnitude M_c depend on which of many published methodologies is used (Ogata & Katsura 1993; Wiemer & Wyss 2000; Cao & Gao 2002; Woessner & Wiemer 2005; Amorèse 2007; Schorlemmer & Woessner 2008; Clauset *et al.* 2009; Corral *et al.* 2011; Mignan *et al.* 2011; Mignan & Woessner 2012; Tormann *et al.* 2014; Corral & González 2019; Lombardi 2021; Taroni *et al.* 2021). Lombardi (2021) reviewed the reliability of these methods in determining accurate statistical properties, highlighting some weak points, largely connected to M_c evaluation. Moreover, she proposed a new method, the Normalized Distance (ND) test, which overcomes these limitations, placing the problem of M_c evaluation into a full statistical testing framework. The novelty of this method consists in the using of a new statistic to check the exponential/geometric distribution of magnitudes, which has the advantage to be independent of the sample size and, therefore, for which the null distribution may be easily computed.

The present study has been undertaken with two main objectives: (1) to refine the Normalized Distance test and (2) to deepen understanding of *b*-value variations during earthquake sequences. In particular, this study tests the hypothesis that many published *b*-value anomalies can arise from a combination of chance and artefacts of the data quality and analysis.

2 REFINING THE NORMALIZED DISTANCE TEST

The detection of anomalies in a *b*-value time-series is usually formulated as identifying outlier data points relative to a reference threshold b_{ref}, which is generally estimated on the background seismicity, as a single regional average or as the median of all individual *b*-values in a time-series. It is, therefore, necessary to define a procedure that, for each step of the time-series, (1) looks for M_c, above which there is no clear evidence for rejection of the hypothesis of an exponential/geometric distribution of magnitudes, a necessary condition for the *b*-value estimator, (2) estimates *b,* conditional on M_c and (3) checks if the relative difference between the estimated *b*-value and b_{ref} is statistically significant.

The first two steps are here made by using the ND test (Lombardi 2021), which is structured as follows.

Given a sample *S* of magnitudes, three quantities are computed, as function of the ascending minimum magnitude *M* (Lombardi 2021):

(1) the geometric maximum likelihood *b*-value estimator $b_{est}(M)$;
(2) the *W*-statistic $W(M) = \sqrt{N} \cdot D[b_{est}(M)]$, where $D[b_{est}(M)]$ is the statistic of the Lilliefors test (Gibbons & Chakraborty 2003) and *N* is the sample size above *M*;
(3) the probability $p_W(M)$ to exceed $W(M)$, under the hypothesis that the magnitudes above *M* follow the GRL with parameter $b_{est}(M)$.

This procedure is repeated for an ensemble of N_B randomly selected bootstrap-resampled catalogues, assuming the same underlying distribution, and the completeness magnitude M_c^B is computed, for each of them, by selecting the lowest magnitude *M* for which $p_W(M) > \alpha$, where α is the prefixed significance level of the test. The empirical distribution of values M_c^B represents the uncertainty about the completeness magnitude M_c of the sample *S*; therefore the $(1 - \alpha) \times 100$ per cent percentile of values M_c^B gives the value of M_c, and then of *b*, for *S*, with a significance level equal to α.

The ND test is based on the computation of the expected distribution of the *W*-statistic, function of b_{est}, but independent of *N*. This distribution may be computed empirically, on simulated data (Lombardi 2021). Any *k*th percentile of *W* (marked by q_W^k) is linearly dependent on b_{est} (Fig. 1), so that we may use the formula $q_W^k = A_1 + A_2 \cdot b_{est}$, to compute them, where A_1 and A_2 are constant. Table 1 lists the values of A_1 and A_2, together with their errors, for some percentiles commonly used for statistical tests. These are empirically estimated by a regression analysis on thousands of synthetic samples, with a size *N* going from 50 to 10^5 and simulated with an assumed *b* ranging from 0.5 to 2.5.

The significance difference between the estimated *b*-value b_{est} and the reference value b_{ref}, is quantified by the log-likelihood ratio (LLR) test (Kalbfleisch 1985), which assesses the goodness of fit of two competing statistical models, having the same numbers of parameters, based on the ratio of their likelihoods.

3 b-VALUE VARIATIONS IN ITALY DURING THE RECENT MAJOR EARTHQUAKE SEQUENCES

To search for any spatio-temporal variation of *b*-value during the recent major seismic sequences in Italy, we performed a spatio-temporal scan of the *b* and M_c parameters using the ND test. This is applied on intersecting samples of N_{tw} events, temporally moved forward by N_s events through the catalogue. Each of them is spatially distributed in subsamples, having locations inside overlapping circles covering the regions under study, with a fixed radius *R* and centres C_j equally spaced at distance *D*. Note that the *b*-value maps are not equally distributed in time, since they follow the temporal evolution of seismicity.

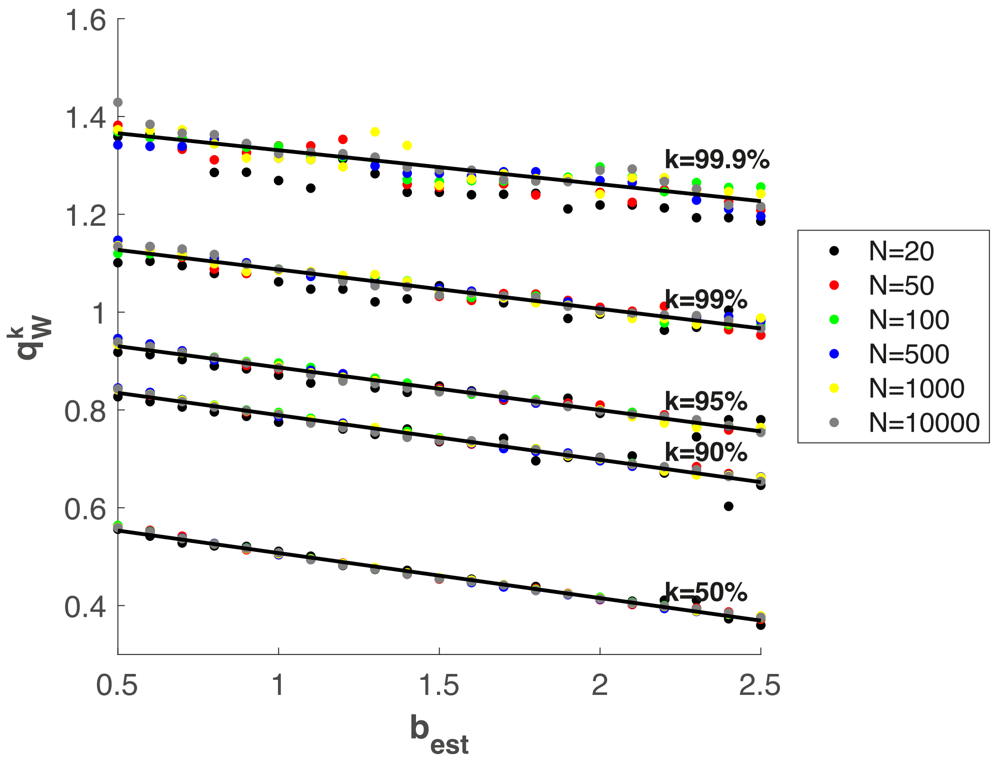

Figure 1. Log linear relation between some percentiles (q_W^k) of *W*-statistic of the ND test and b_{est}, for different percentages (indicated on the right-hand side of the picture). The values of q_W^k are empirically computed from hundreds of thousands geometric simulated samples, for different values of *b* and of sample size *N*. Black solid lines mark the linear relations obtained by regression analyses of which coefficients are listed in Table 1.

Table 1. Coefficients (with the standard errors in the brackets) of the linear relation between some percentiles of *W* and b_{est}.

Percentile	A_1	A_2
90 per cent	8.80e-01 (1.0e-03)	−9.1e-02 (1.0e-03)
95 per cent	9.70e-01 (1.0e-03)	−8.7e-02 (1.0e-03)
99 per cent	1.17 (2.0e-03)	−8.0e-02 (1.0e-03)
99.9 per cent	1.40 (5.0e-03)	−6.9e-02 (3.0e-03)

The *b*-value estimation is particularly sensitive to the magnitude range (ΔM) covered by data (Geffers *et al.* 2022): strongly biased values may be obtained for low (where 'low' depends on *b*) magnitude ranges and small sample sizes (Supporting Information Fig. S1). As a result of this analysis we recommend using samples that a) cover a magnitude range $\Delta M > 1.5/b$, to avoid overestimated *b*-values and b) have more than 50 events above M_c, to avoid underestimated *b*-values, for large ΔM.

We choose a significance level $\alpha = 0.01$ for the ND and LLR tests, in the following analysis. The empirical probability distribution for M_c is estimated on 10^5 bootstrap resamples, so that the 99th percentile is computed from 10^3 values, and hence is a robust estimate.

Since 2005, two Italian regions were struck by three seismic sequences, with the larger events having local magnitudes $M_L \geq 5.5$ (Fig. 2). The first is the Emilia region (ER; [10.60–11.90E, 44.50–45.30N]) with a single sequence in 2012, containing a main event occurring on 2012 May 12, in Finale Emilia, with magnitude M_L5.9. The second region is the Central Italy region (CIR; [12.7–13.80E, 42.00–43.30 N]), with two sequences in 2009 (main event 2009 April 6, L'Aquila, M_L5.9) and in 2016–2017 (main event 2016 October 30, Norcia, M_L6.1). The detection magnitude of the INGV National Seismic Network is close to M_L1.5, for the CIR, and to M_L2.0 for the ER (Schorlemmer *et al.* 2010). The events collected in the Italian Seismic Bulletin (BSI, Bollettino Sismico Italiano; http://terremoti.ingv.it/en/iside; http://terremoti.ingv.it/en/bsi) of the Istituto Nazionale di Geofisica e Vulcanologia, with depth above 30 km and magnitude above the detection levels, since 2005 April 16 (when the completely re-organized National Seismic Network of the INGV came into operation; Amato & Mele 2008) to 2021 April 30, are 69 460 and 2502, in the CIR and ER, respectively.

The study of *b*-value variations in these regions is of interest for several reasons. The 2009 L'Aquila main shock was preceded by about 3 months of seismicity, largely confined to a patch close to the main-shock nucleation point, for which a low *b*-value was recognized and retrospectively correlated to a highly stressed zone (DeGori *et al.* 2012; Sugan *et al.* 2014; Gulia *et al.* 2016). The 2009 L'Aquila earthquake was, therefore, included in cases where the *b*-value decrease is interpreted as a precursor to a strong event (Papadopoulos *et al.* 2010; Gulia *et al.* 2016). The 2012 Emilia sequence was thought to be originated by movement on thrust faults, which are thought to be associated with lower *b*-values than for normal faulting (Schorlemmer *et al.* 2005). Finally, the 2016 Norcia earthquake (2016 October 30) was preceded by subsequently identified foreshocks, reaching magnitude M_L6.0 with the Amatrice earthquake (2016 August 24), for which a drop of *b*-value was recognized and proposed as a useful mean to distinguish, in real time, potential foreshocks to an upcoming larger event (Gulia & Wiemer 2019).

We now assess the significance of these inferences based on the procedure outlined in section 2. First, we carried out a spatiotemporal scan of M_c and *b* by applying the ND-test on the seismicity of the ER and CIR, above the minimum magnitude M_{min}. As

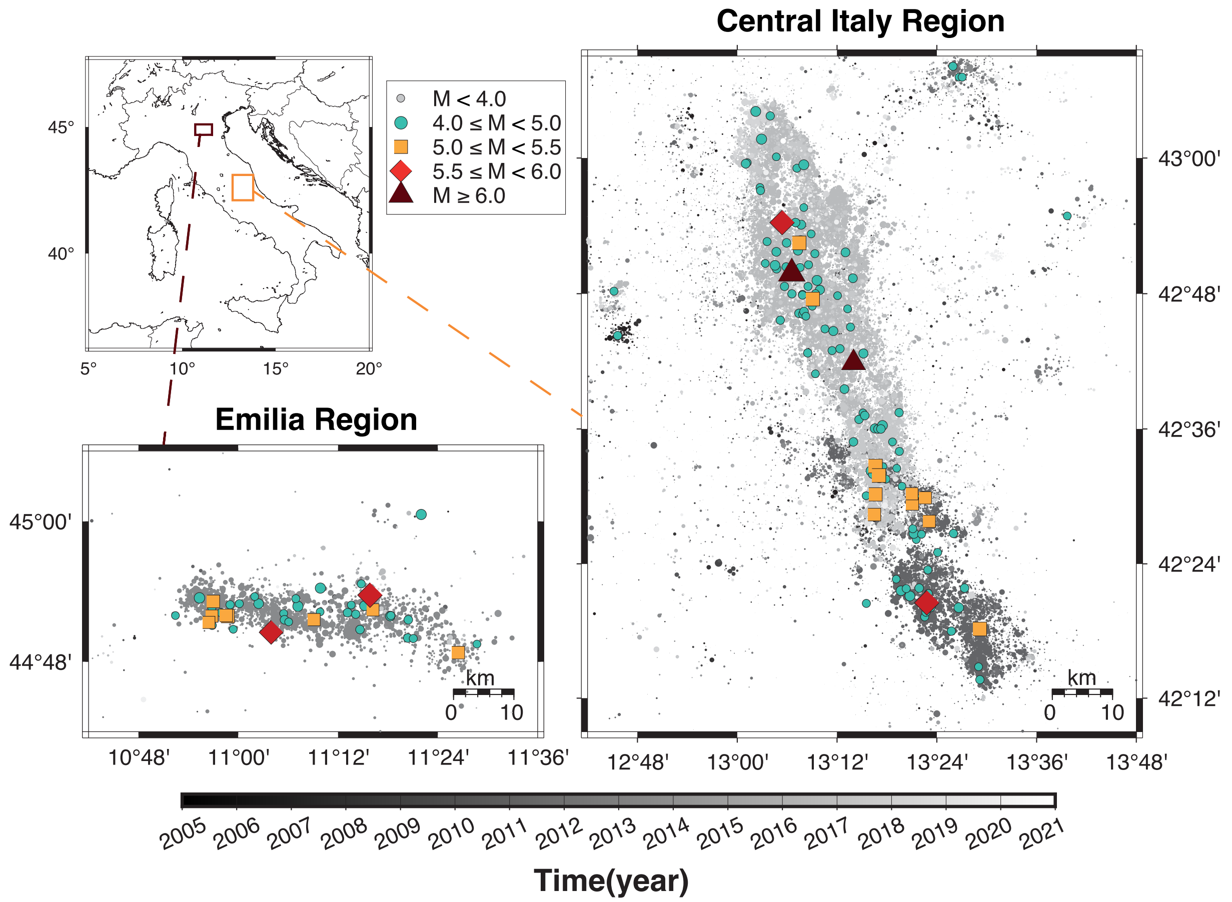

Figure 2. Map of the events occurred in the Emilia and the Central Italy regions, from 2005 April 16 to 2021 April 30, above 30 km of depth and with magnitudes above M_L2.0 and M_L1.5, respectively. The symbol size is scaled with magnitude. The grey colour marks the events below M_L4.0 and is scaled with the occurrence time.

Table 2. Parameters used for the spatio-temporal scan of b and M_c.

	Emilia		Central Italy	
M_{min}: minimum magnitude	2.0		1.5	
N_{min}: minimum sample size (above M_c)	50		50	
N_{tw} number of events for each time window	Reference Seismic sequence	All 250 and 500	Reference Seismic sequences	500 and 1000 250 and 500
N_s number of events for the time window shift	10		10	
R radius (in km) for the spatial scan	Reference Seismic sequence	All 5 and 10	Reference Seismic sequences	10 5 and 10
D spatial shift (in degree) of the samples	0.025°		0.025°	
α significance level of the ND and LLR tests	0.01		0.01	
$NSIM$ number of simulations to compute the p-values of the ND test	10^5		10^5	

said above, this last is taken from the study of earthquake detection capabilities of the Italian National Seismic Network made by Schorlemmer *et al.* (2010). Table 2 lists the values of parameters used in this analysis.

Most of the seismicity of the ER belongs to the first month of the 2012 sequence: 60 events (maximum magnitude $M_{max} = 4.8$) were recorded before 2012 May 18 (the start date of the 2012 sequence) and 230 events ($M_{max} = 4.5$) after 01 January 2013. Given the constraint of $N_{min} > 50$, only a single global b-value may be estimated from these data. The ND test provides (a) $M_c = 2.2$ (42 events) and $b_{est} = 1.0$ (s.d. 0.2), for the first sample; (b) $M_c = 2.6$ (53 events) and $b_{est} = 1.1$ (s.d. 0.1), for the second and (c) $M_c = 2.6$ (69 events) and $b_{est} = 1.1$ (s.d. 0.1) for the joint samples (Supporting Information Fig. S2). The choice of the reference b-value is driven by the same rationale adopted in the following: a b-value is equal to 1.0, unless the LLR test rejects this hypothesis. The final $b_{est}$is not statistically different from 1.0, by the LLR test (p-value = 42 per cent). So, $b_{ref} = 1.0$ is assumed as the reference b-value of the ER. The subsamples with $\Delta M < 1.5$ are ruled out by the analysis to avoid overestimation of b-value for small magnitude ranges (Geffers *et al.* 2022; Supporting Information Fig. S1).

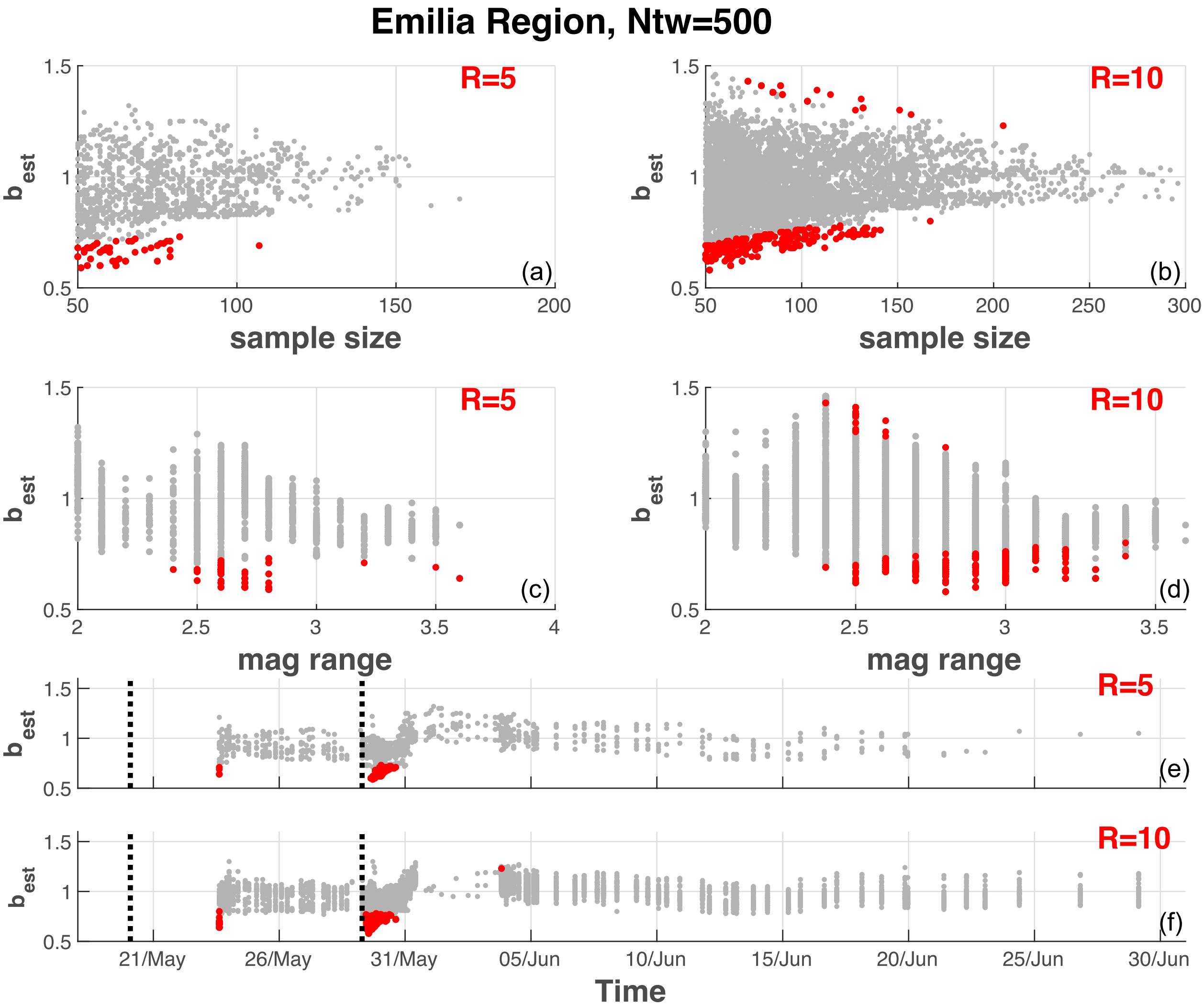

Figure 3. *b*-Value analysis, during the first months of the 2012 Emilia sequence (2012 May 18–December 31), by applying the ND test with $N_{tw} = 500$. (a) Estimated *b*-values versus the sample size, for $R = 5$ km. The red points mark the *b*-values significantly different from $b_{ref} = 1.0$. (b) The same as (a), but for $R = 10$ km. (c) Estimated *b*-values versus the magnitude range, for $R = 5$ km. (d) The same as (c), but for $R = 10$ km. (e) Time-series of the estimated *b*-values (for the period 2012 May 18–June 30) for $R = 5$ km; time indicates the end of the temporal interval of the sample. The red points mark the *b*-values significantly different from $b_{ref} = 1.0$. The vertical dotted black lines mark the occurrence of the two major earthquakes (20 May, M_L5.9 and 29 May, M_L5.8). (f) The same as (e), but for $R = 10$ km.

The analysis of the ER seismicity from 2012 May 18 to December 31 provides significant (p-value < 0.01) departures of *b*-value from the reference $b_{ref} = 1.0$, soon after the occurrence of two main events, having magnitude $M_L \geq 5.5$ (2012 May 20, Finale Emilia, M_L5.9; 2012 May 29, Medolla, M_L5.8; Supporting Information Fig. S3), when the completeness of the seismic catalogue is strongly affected by the changes in the recording seismic network and limitations in detection, due to overlapping seismograms for different events (Peng *et al.* 2007). By removing the seismicity within 12 hr after the occurrence of two main shocks, the anomalous *b*-values disappear. No anomaly is observed before the occurrence of main events All the maps of M_c and b_{est} are shown in the Supporting Information (Movie S1).

The estimation of b_{ref} for the CIR is done by computing the median of individual *b*-values in a time-series. To this end, the seismicity occurring out of the most intense phases of both 2009 L'Aquila and 2016 Central Italy sequences is selected and divided in three periods: *P*1*,* 2005 April 16–2008 December 31; *P*2*,* 2011 January 1–2016 August 18 and *P*3, 2019 January 1–2021 April 30. The spatio-temporal scan of the selected seismicity (by using the parameters listed in Table 2) gives values of b_{est} with overall median values of 1.0 and 1.1, for $N_{tw} = 1000$ and 500, respectively (Supporting Information Fig. S4), steady for a lower threshold of ΔM equal to 1.5 or more. In the following, the analysis of *b*-value anomalies with respect to the null hypothesis $b_{ref} = 1.0$, for samples with $\Delta M > 1.5$, is shown. However, the results are not sensitive to this choice, at least if $b_{ref} = 1.1$.

Once again, anomalously low *b*-values with respect to $b_{ref} = 1.0$ are detected soon after the occurrence of the main events of the 2009 L'Aquila (2009 April 6, M_L5.9; Supporting Information Figs S4 and S5) and 2016–2017 Central Italy (2016 August 24, M_L6.0; 2016 October 26 M_L5.9; 2016 October 30 M_L6.1) sequences. Moreover, some anomalies are recognized at 2017 January 18, when four events with $M_L > 5.0$ occurred within about 4 hr (Supporting Information Figs S5 and S6). Again, the anomalies disappear after removing the events in the first 24 hr after the main events. All maps

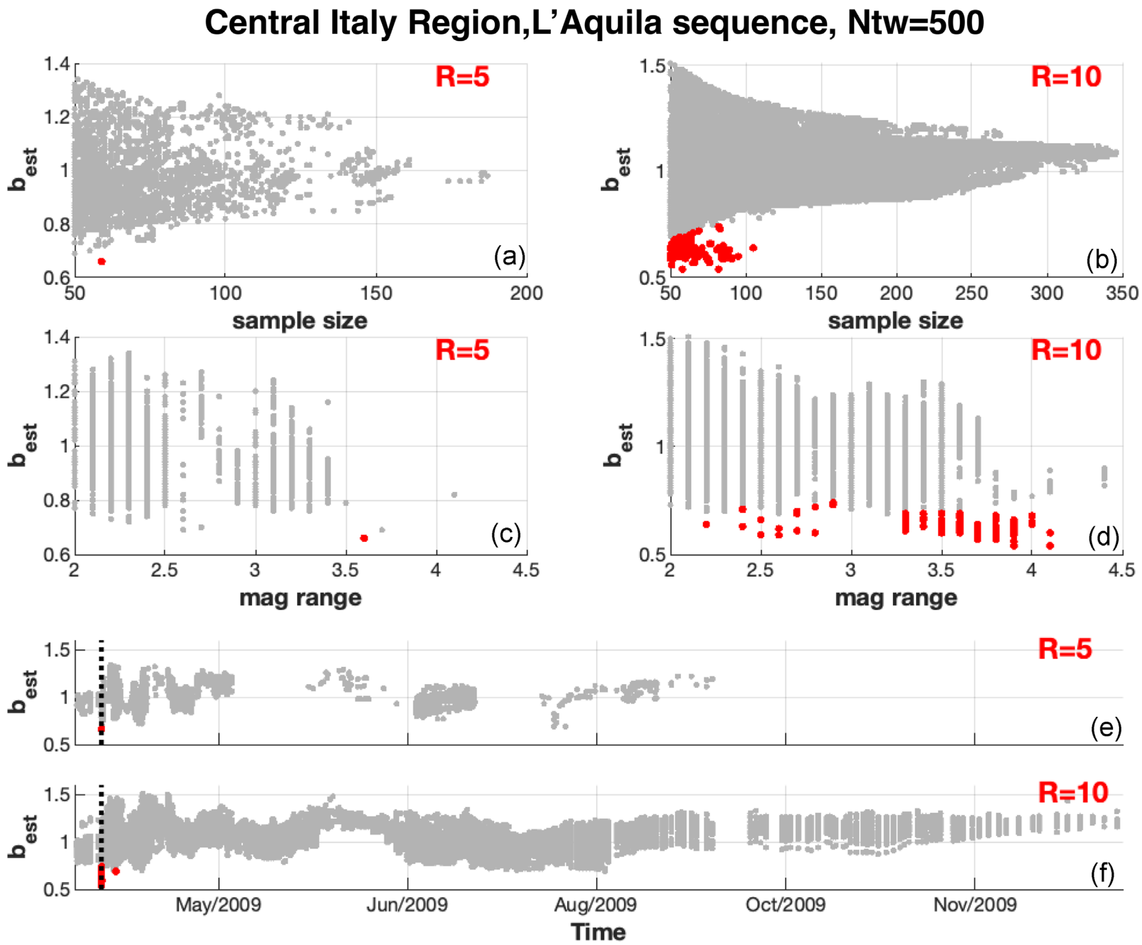

Figure 4. *b*-Value analysis of the 2009 L'Aquila sequence seismicity (2009 January 1–2010 December 31), by applying the ND test with $N_{tw} = 500$. (a) Estimated *b*-values versus the sample size for $R = 5$ km. The red points mark the *b*-values significantly different from $b_{ref} = 1.0$. (b) The same as (a), but for $R = 10$ km. (c) Estimated *b*-values versus the magnitude range cover by the sample, for $R = 5$ km. (d) The same as (c), but for $R = 10$ km. (e) Time-series of the estimated *b*-values (for the period 2009 March 30–December 31) for $R = 5$ km; time indicates the end of the temporal interval. The red points mark the *b*-values significantly different from $b_{ref} = 1.0$. The vertical dotted black lines mark the occurrence of the major earthquake (2009 April 6, M_L5.9). (f) The same as (e), but for $R = 10$ km.

of M_c and b_{est} are shown in the Supporting Information (Movies S2 and S3).

4 DISCUSSION

This paper deals with the age-old topic of establishing *b*-value variations and their effect on the short-term seismic risk, just before and during a seismic sequence (Schorlemmer & Wiemer 2005; De Gori *et al.* 2012; Sugan *et al.* 2014; Tormann *et al.* 2014; Gulia *et al.* 2016; Gulia & Wiemer 2019). The core of this study concerns (1) to find *b*-value changes, by the ND test, during the recent main sequences in Italy, and (2) to discuss possible statistical factors that may interfere with the detection of *b*-values anomalies.

All the anomalous low *b*-values, recognized in this study for the ER and CIR by the ND test, are due to the incompleteness and heterogeneity of seismicity, due to overlapping seismograms for consecutive events (Peng *et al.* 2007), immediately following a large event or close together, moderate earthquakes (Figs 3–5). By removing this seismicity, the anomalies disappear. Remarkably, no significant *b*-value decrease is found before the occurrence of any largest events, contrary to similar analyses, not using the procedures outlined here to determine M_c, that attribute statistical significance and hence predictive power to a drop in *b*-value, particularly for the 2009 L'Aquila and 2016 Central Italy sequences (Papadopoulos *et al.* 2010; De Gori et al 2012; Gulia *et al.* 2016; Gulia & Wiemer 2019). This conclusion agrees with what reached by the IASPEI exercise on significant precursors (Wyss 1997) and the review on operational earthquake forecasting (Jordan *et al.* 2011), both stating that the search for precursory *b*-value anomalies (as well as for any other precursor) has not yet produced a successful short-term prediction scheme. Once again, the rise of *b*-value during the immediate aftershock sequences may be attributed to the increase of M_c, with a consequent decrease of ΔM (Fig. 6b), caused by overlapping events (Peng *et al.* 2007; Supporting Information Fig. S7). Finally, no significant difference of absolute *b*-value is found between the compressive, Emilia, and the estensive, Central Italy, regions.

A detailed comparison with cited published analyses on *b*-value changes is not an aim of this study, but several statistical reasons may be hypothesized for the difference between our results and those of Papadopoulos *et al.* (2010), De Gori et al (2012), Gulia *et al.* (2016) and Gulia & Wiemer (2019), in terms of the significance of changes in *b*-value. To investigate this question, we compare

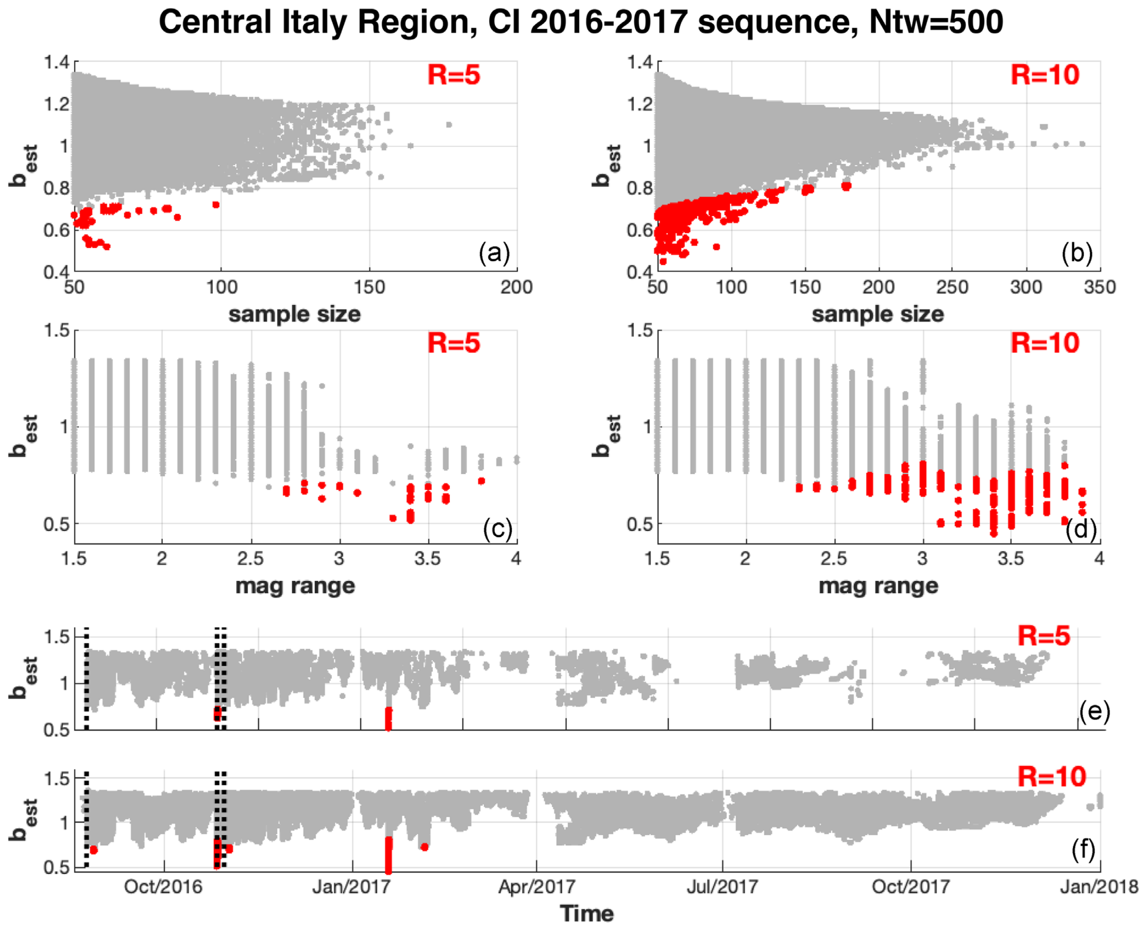

Figure 5. *b*-value analysis of the 2016 Central Italy sequence seismicity (2016 August 18–2018 December 31), by applying the ND test with $N_{tw} = 500$. (a) Estimated *b*-values versus the sample size for $R = 5$ km. The red points mark the *b*-values significantly different from $b_{ref} = 1.0$. (b) The same as (a), but for $R = 10$ km. (c) Estimated *b*-values versus the magnitude range cover by the sample, for $R = 5$ km. (d) The same as (c), but for $R = 10$ km. (e) Time-series of the estimated *b*-values (for the period 2016 August 18–2017 December 37) for $R = 5$ km; time indicates the end of the temporal interval. The red points mark the *b*-values significantly different from $b_{ref} = 1.0$. The vertical dotted black lines mark the occurrence of the major earthquakes (2016 August 24, M_L6.0; 2016 October 26, M_L5.9; 2016 October 30, M_L6.1). f) The same as (e), but for $R = 10$ km.

pure results using the ND test with those obtained by a commonly applied method of determining M_c and *b*-value (called MAXC-NLI in the following) that (1) estimates M_c by the maximum curvature method (MAXC; Wiemer & Wyss 2000), with a correction factor of 0.2 and 0.4 for the background and the sequences, respectively (Gulia & Wiemer 2019); (2) applies the linearity test (Tormann *et al.* 2014) and (3) uses the maximum likelihood estimator from an exponential distribution to estimate *b*. Samples with less than 50 events, above M_c, are ruled out, to allow a like for like comparison. This comparison is done to highlight some issues of paramount importance for the estimation of M_c and *b* parameters, discussed in the following (Fig. 6).

(1) *The estimation of* b_{ref} *and the correlation between* b_{est} *and* ΔM. The *b*-value anomalies are detected with respect to a reference level b_{ref}, which is generally estimated from the background seismicity, as a single regional overall value or as the median of all individual *b*-values in a time-series. Fig. 6(a) shows the values of *b*, obtained by applying the MAXC-NLI method, on seismicity that occurred in CIR and during the three background periods *P*1, *P*2 and *P*3, set before. The overall median *b*-value is equal to 1.3, significantly larger than that obtained by the ND test (Supporting Information Fig. S4). This difference is due to the high proportion (likely for the background seismicity) of subsamples with joined small size and small magnitude range (more than 60 per cent of samples has less than 100 events and $\Delta M < 1.5$), for which the estimator of *b* is biased (Supporting Information Fig. S1; Geffers *et al.* 2022). So much so that, the median of b_{ref} values decreases to 1.1 if samples with $\Delta M \geq 1.5$ are selected.

The effects of an overestimated b_{ref} can be illustrated by analysing, as an example, the seismicity around (10 km of radius) the 2016 Norcia earthquake location. The value of b_{ref} for this region goes from 1.3 to 1.0, by increasing the lower threshold for ΔM up to 1.9 or more. The time-series of *b*-values (Fig. 6b) shows anomalously low *b*-values, between the 2016 Amatrice and the Norcia earthquakes, only if you consider $b_{ref} = 1.3$. Moreover, the *b*-values are, once again, inversely related to ΔM, so that the higher *b*-values, observed after the occurrence of the main event, corresponds to $\Delta M < 1.8$.

The movies collecting all maps of the estimated M_c and *b* (Supporting Information Movies S1–S3) definitely show the relation between these two parameters: b_{est} values are significantly smaller (p-value < 0.01) than the reference value where the M_c values increase (and ΔM decreases), as effect of the occurrence of strong events.

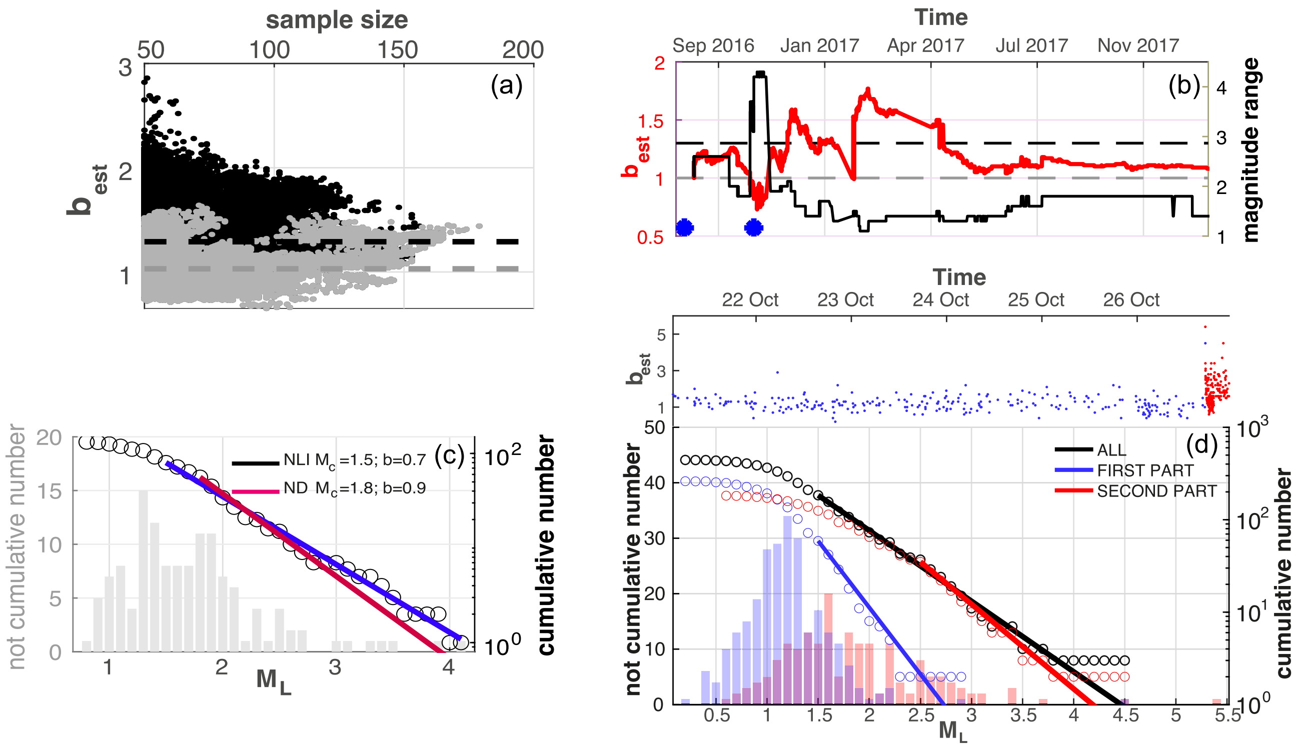

Figure 6. Possible causes of misunderstood b-value anomalies. (a) Comparison of b-value estimations (points) and overall median value (dashed lines), provided by the MAXC-NLI method for the definition of b_{ref} in the CIR. The black colour marks data without a threshold for ΔM. The grey colour refers to subset of data with $\Delta M > 1.5$. (b) Values of b_{est} (red solid line) and ΔM (black solid line) obtained by the MAXC-NLI method, around the Norcia earthquake location, during the 2016 CI sequence. Blue stars mark the occurrence of Amatrice and Norcia earthquakes. Black and grey dashed lines mark the b_{ref} value obtained without and with a minimum threshold for ΔM. (c) Different estimation of M_c for seismicity of the last week before and around the 2009 L'Aquila earthquake. The grey histogram refers to the number of events per magnitude bin. The black circles mark the cumulative number of events per magnitude bin. The red and blue solid lines mark the GRL estimation by the ND and MAXC-NLI methods, respectively. (d) Variation of M_c from 1.5 (blue dots) to 2.5 (red dots) inside a sample. The blue and red histograms refer to the number of events per magnitude bin, for the first and the second part of the sample, respectively. The blue and red circles mark the cumulative number of events per magnitude bin, for the first and the second part of the sample, respectively. The blue and red solid lines mark the GRL estimation by the ND method, for the first and the second part of the sample, respectively. The black circles mark the overall cumulative number of events per magnitude bin. The black solid line marks the GRL estimation by the ND method for the whole sample.

(2) *Not exponential/geometric data and underestimation of* M_c. Most of published methods hides a discrepancy between the M_c evaluation, based on the departure of the logarithmic cumulative magnitude frequency from a linear behavior, and the b-value estimation, based on the hypothesis of an exponential/geometric distribution for magnitudes (Lombardi 2021). Exponential/geometric magnitudes have undoubtedly a log-linear cumulative distribution, but the reverse is a bit trickier question.

An example of misestimation of M_c is shown in Fig. 6(c) and refers to foreshocks of the last week before the 2009 L'Aquila event, for which an anomalous low b-value was recognized (Papadopoulos *et al.* 2010; Gulia *et al.* 2016). The MAXC-NLI method gives lower values of both M_c and b, respect to the ND test, because the incompleteness of the lower portion of the magnitude range is not captured by the NLI test. Leaving aside the significance of this difference, this example shows that anomalous low b-values may be due to an underestimation of M_c, and hence an artefact.

(3) *Variation of* M_c *inside the sample*. The spatial-temporal scan of b-value requests the choice of a sampling step to divide the available data in subsamples. This step, however chosen, might identify subsets of data with inside a temporally or spatially variable (heterogeneous) M_c. Fig. 6(d) shows an example concerning a subset of events, occurred from 21 to 27 October around Norcia. The occurrence of two close events at 26 October (Castelsantangelo sul Nera, M_L5.4 and Visso, M_L5.8) leads to overlapping seismograms that hide small events, causing an increase of M_c (from M_L1.5 to M_L2.5). The overall sample is wrongly interpreted, by the ND method, as an exponential sample with a completeness $M_c = 1.5$, actually valid only for the first part of the sample, and a low b-value, due to the lack of events below 2.5 in the second part of the sample and to the consequent biased proportion between the small and the large events for the overall sample.

(4) *Significance of b-value variations*. The detection of b-value anomalies is essentially based on the measure of the significance of relative b-value differences. To discuss good and bad points of published methods measuring this significance is beyond the aims of this study. The key issue is that the practice of using a fixed percentage change as a threshold for identifying an abnormal b-value performs poorly because the significance of b-value differences depends on some inter-related factors, as chance, bias, sample size and magnitude range.

Our findings are based on the hypothesis of validity of the GRL for magnitudes, at all scales. This hypothesis was been challenged recently for low magnitudes, in high-resolution earthquake catalogues, mostly due to problems in recording and processing procedures (Hermann & Marzocchi 2021). This suggests as the maximum caution must be exercised, for estimating any property of the magnitude distribution, to prevent any misunderstanding.

5 CONCLUSIONS

Using the ND test (Lombardi 2021), the variations in *b*-value during the recent major sequences in Italy are investigated. In contrast with previous studies, no firm evidence for the decrease of the *b*-value before the main shocks is found. The decrease of *b*-value as a precursor to a strong event appears to be less common and more questionable than the literature suggests. It is important to note that most investigations are based on the relative difference of *b*-values, without considering all factors that play an important role on their statistical significance. In particular, misleading conclusions may be produced both by data features (as low sample size, small magnitude range or inhomogeneities in the catalogue) and details of methodologies (e.g. incorrect M_c estimation or b_{ref} overestimation).

We do not reject the hypothesis of the existence of *b*-value precursors, but our results imply that, if they do exist, they are probably overrated (Amorese *et al.* 2010). No method can probably eliminate all bias coming from data. However, an objective judgement of investigation methods, together with a careful analysis of results, may substantially reduce, if not eliminate, misunderstanding arising from artefacts, variability in data quality and the methods of inference. On the other hand, the results concerning the low number of cases dealt in this study, confined in the same small partial region, can only have a local relevance. Therefore, more studies need to be conducted, on a larger population of cases, to strengthen and generalize the validity of these findings.

ACKNOWLEDGMENTS

Maps were prepared with the GMT software package (Wessel & Smith 1991). Calculations for the MAXC-NLI method were performed using the MATLAB codes available from https://doi.org/10.3929/ethz-b-000357449, under the General Public License, in supplement to Gulia & Wiemer (2019).

The author is grateful to reviewers (D. Amorése and I. Main) and the associate editor (M. Segou) for their helpful reviews of the paper.

DATA AVAILABILITY

The parameters of the earthquakes recorded by the Italian Seismic Network, located in the INGV monitoring room in Rome and revised by the Italian Seismic Bulletin (BSI), are available in the Italian Seismological Instrumental and parametric database (ISIDe, http://terremoti.ingv.it/en/iside), in the time frame between 1985 January 1 and today. Starting from 2015, quarterly releases of BSI are published on the web page http://terremoti.ingv.it/en/bsi in QuakeML format and with a DOI assigned.

REFERENCES

Aki, K., 1965. Maximum likelihood estimate of b in the formula log (N) = a − bM and its confidence limits, *Bull. Earthq. Res. Inst. Tokyo Univ.,* **43**(2), 237–239.

Amato, A. & Mele, F. M., 2008. Performance of the INGV national seismic network from 1997 to 2007, *Ann. Geophys.,* **51**(2/3), 99–113.

Amitrano, D., 2003. Brittle-ductile transition and associated seismicity: experimental and numerical studies and relationship with the b value, *J. geophys. Res.,* **108,** 2044.

Amorèse, D., 2007. Applying a change-point detection method on frequency–magnitude distributions, *Bull. seism. Soc. Am.,* **97**(5), 1742–1749.

Amorèse, D., Grasso, J.R. & Rydelek, P.A., 2010. On varying *b*-values with depth: results from computer-intensive tests for Southern California, *Geophys. J. Int.,* **180**(1), 347–360.

Bender, B., 1983. Maximum likelihood estimation of b values for magnitude grouped data, *Bull. Seismol. Soc. Am.,* **73**(3), 831–851.

Cao, A. & Gao, S.S., 2002. Temporal variation of seismic *b*-values beneath northeastern Japan island arc, *Geophys. Res. Lett.,* **29**(9), 48–41-48-3.

Clauset, A., Shalizi, C.R. & Newman, M.E.J., 2009. Power-law distributions in empirical data, *SIAM Rev.,* **51**(4), 661–703.

Corral, A., Font, F. & Camacho, J., 2011. Non-characteristic half-lives in radioactive decay, *Phys. Rev. E,* **83,** 66103.

Corral, A. & González, A., 2019. Power law distributions in geoscience revisited, *Earth Space Sci.*, **6,** 673–697.

De Gori, P., Lucente, F.P., Lombardi, A.M., Chiarabba, C. & Montuori, C., 2012. Heterogeneities along the 2009 L'Aquila normal fault inferred by the *b*-value distribution, *Geophys. Res. Lett.,* **39,** 1–5.

Fielder, G., 1974, Local *b*-values to seismicity, *Tectonophysics,* **23,** 277–282.

Geffers, G., Main, I.G. & Naylor, M., 2022. Biases in estimating *b*-values from small earthquake catalogues: how high are high *b*-values?, *Geophys. J. Int.,* **229,** 1840–1855.

Gibbons, J.D. & Chakraborty, S., 2003. *Nonparametric statistical inference (4th ed., Vol. 36).* :(**Vol. 36,** 4th ed.), Marcel Dekker Inc., New York, NY.

Gibowicz, S.J., 1973. Variation of the frequency–magnitude relation during earthquake sequences in New Zealand, *Bull. seism. Soc. Am.,* **63**(2), 517–528.

Goebel, T. H. W., Becker, T. W., Schorlemmer, D., Stanchits, S., Sammis, C., Rybacki, E. & Dresen, G., 2012. Identifying fault heterogeneity through mapping spatial anomalies in acoustic emission statistics, *J. geophys. Res.,* **117,** B03310, doi:10.1029/2011JB008763.

Gulia, L., Tormann, T., Wiemer, S., Herrmann, M. & Seif, S., 2016. Short-term probabilistic earthquake risk assessment considering time-dependent *b* values, *Geophys. Res. Lett.,* **43,** 1100–1108.

Gulia, L. & Wiemer, S., 2019. Real-time discrimination of earthquake foreshocks and aftershocks, *Nature,* **574**(7777), 193–199.

Gutenberg, B. & Richter, C. F., 1942. Earthquake magnitude, intensity, energy, and acceleration, *Bull. seism. Soc. Am.,* **32**(3), 163–191.

Herrmann, M. & Marzocchi, W., 2021. Inconsistencies and lurking pitfalls in the magnitude–frequency distribution of high-resolution earthquake catalogs, *Seismol. Res. Lett.,* **92,** 909–922.

Ishimoto, M. & Iida, K., 1939. Observations of earthquakes registered with the microseismograph constructed recently, *Bull. Earthq. Res. Inst. Univ. Tokyo,* **17,** 443–478.

Jordan, T. *et al.*, 2011. Operational earthquake forecasting: state of knowledge and guidelines for utilization, *Ann. Geophys.,* **54**(4), 361–391.

Jordan, T. H., 2006. Earthquake predictability, brick by brick, *Seismol. Res. Lett.,* **77**(1), 3–6.

Kagan, Y., 1999. The universality of the frequency-moment relationship, *Pure appl. Geophys.,* **155,** 537–574.

Kalbfleisch, J. G., 1985. *Probability and Statistical Inference (Volume 2: Statistical Inference),* 2nd edn, Springer-Verlag, pp. 1–360.

Kamer, Y. & Hiemer, S., 2015, Data-driven spatial bvalue estimation with applications to California seismicity: to b or not to b, *J. geophys. Res.,* **120,** 5191–5214.

Kun, F., Varga, I., Lennartz-Sassinek, S. & Main, I., 2013. Approach to failure in porous granular materials under compression, *Phys. Rev. E,* **88**(6), 062207.

Lombardi, A.M., 2021. A normalized distance test for co-determining the completeness magnitude and *b*-value of earthquake catalogs, *J. geophys. Res.,* **126,** e2020JB021242.

Main, I. G., Meredith, P. G. & Jones, C., 1989. A reinterpretation of the precursory seismic *b*-value anomaly from fracture mechanics, *Geophys. J. Int.,* **96**(1), 131–138.

Main, I. G., Meredith, P. G. & Sammonds, P. R., 1992. Temporal variations in seismic event rate and *b*-values from stress corrosion constitutive laws, *Tectonophysics,* **211**(1), 233–246.

Main, I., 2000. Apparent breaks in scaling in the earthquake cumulative frequency–magnitude distribution: fact or artifact?, *Bull. seism. Soc. Am,* **90**(1), 86–97.

Marzocchi, W. & Sandri, L., 2003. A review and new insights on the estimation of the *b*-value and its uncertainty, *Ann. Geophys.,* **46,** 1271–1282.

Marzocchi, W., Spassiani, I., Stallone, A. & Taroni, M., 2020, How to be fooled searching for significant variations of the b-value, *Geophys. J. Int.,* **220**(3), 1845–1856.

Mignan, A., Werner, M.J. Wiemer, S. Chen, C.-C. & Wu, Y.-M. 2011. Bayesian estimation of the spatially varying completeness magnitude of earthquake catalogs, *Bull. Seismol. Soc. Am.,* **101,** 1371–1385, doi:10.1785/0120100223.

Mignan, A. & Woessner, J., 2012. Estimating the magnitude of completeness for earthquake catalogs, *Community Online Resource for Statistical Seismicity Analysis,* available at http://www.corssa.org (accessed: 20/06/2022).

Mogi, K., 1962. Study of the elastic shocks caused by the fracture of heterogeneous materials and its relation to earthquake phenomena, *Bull. Earthq. Res. Inst.,* **40,** 125–173.

Mogi, K., 1979. Two kinds of seismic gaps, *Pure appl. Geophys.,* **117,** 1172–1186.

Ogata, Y. & Katsura, K., 1993. Analysis of temporal and spatial heterogeneity of magnitude frequency distribution inferred from earthquake catalogs, *Geophys. J. Int.,* **113,** 727–738.

Oncel, A.O. & Wilson, T., 2007. Anomalous seismicity preceding the 1999 Izmit event, NW Turkey, *Geophy. J. Int.,* **169**(1), 259–270.

Papadopoulos, G. A., Charalampakis, M., Fokaefs, A. & Minadakis, G., 2010. Strong foreshock signal preceding the L'Aquila (Italy) earthquake (M_w 6.3) of 6 April 2009, *Nat. Hazards Earth Syst. Sci.,* **10,** 19–24.

Peng, Z., Vidale, J.E., Miaki, M. & Helmstetter, A., 2007. Seismicity rate immediately before and after main shock rupture from high-frequency waveforms in Japan, *J. geophys. Res.,* **112,** B03306.

Rundle, J.B., Klein, W., Turcotte, D.L. & Malamud, B.D., 2000. Precursory seismic activation and critical-point phenomena, *Pure appl. Geophys.,* **157,** 2165–2182.

Scholz, C. H., 1968. The frequency—magnitude relation of microfracturing in rock and its relation to earthquakes, *Bull. seism. Soc. Am.,* **58,** 399–415.

Schorlemmer, D., Mele, F. & Marzocchi, W., 2010. A completeness analysis of the national seismic network of Italy, *J. geophys. Res.,* **115,** B04308, doi:10.1029/2008JB006097.

Schorlemmer, D. & Wiemer, S., 2005. Microseismicity data forecast rupture area, *Nature,* **434,** 1086.

Schorlemmer, D., Wiemer, S. & Wyss, M., 2005. Variation in earthquake-size distribution across different stress regimes, *Nature,* **437,** 539–542.

Schorlemmer, D. & Woessner, J., 2008. Probability of detecting an earthquake, *Bull. seism. Soc. Am.,* **98**(5), 2103–2117.

Schurr, B. *et al.*, 2014. Gradual unlocking of plate boundary controlled initiation of the 2014 Iquique earthquake, *Nature,* **512,** 299–302.

Smith, W. D., 1981. The *b*-values as an earthquake precursor, *Nature,* **289,** 136–139.

Smith, W.D., 1986. Evidence for precursory changes in the frequency–magnitude *b*-value, *Geophys. J. Int.,* **86**(3), 815–838.

Smith, W.D., 1998. Resolution and significance assessment of precursory changes in mean earthquake magnitudes, *Geophys. J. Int.,* **135,** 515–522,

Sugan, M., Kato, A., Miyake, H., Nakagawa, S. & Vuan, A., 2014. The preparatory phase of the 2009 M_w6.3 L'Aquila earthquake by improving the detection capability of low-magnitude foreshocks, *Geophys. Res. Lett.,* **41,** 6137–6144.

Suyehiro, S., 1966. Difference between aftershocks and foreshocks in the relationship of magnitude to frequency of occurrence for the great chilean earthquake of 1960, *Bull. seism. Soc. Am.,* **56**(1), 185–200.

Taroni, M., Marzocchi, W., Schorlemmer, D., Werner, M.J., Wiemer, S., Zechar, J.D., Heiniger, L. & Euchner, F., 2018. Prospective CSEP Evaluation of 1-Day, 3-Month, and 5-Yr Earthquake Forecasts for Italy, *Seism. Res. Lett,* **89**(4). 1251–1261.

Taroni, M., Zhuang, J. & Marzocchi, W., 2021. High-Definition mapping of the Gutenberg–Richter *b*-value and its relevance: a case study in Italy, *Seismol. Res. Lett.,* **92**(6), 3778–3784, .

Tinti, S. & Mulargia, F., 1987. Confidence intervals of *b*-values for grouped magnitudes, *Bull. seism. Soc. Am.,* **77,** 2125–2134.

Tormann, T., Enescu, B., Woessner, J. & Wiemer, S., 2015. Randomness of megathrust earthquakes implied by rapid stress recovery after the Japan earthquake, *Nat. Geosci.,* **8,** 152–158.

Tormann, T., Wiemer, S. & Hardebeck, J., 2012. Earthquake recurrence models fail when earthquakes fail to reset the stress field, *Geophys. Res. Lett.,* **39,** L18310, doi:10.1029/2012GL052913.

Tormann, T., Wiemer, S. & Mignan, A., 2014. Systematic survey of high-resolution b value imaging along Californian faults: inference on asperities, *J. geophys. Res.,* **119,** 2029–2054.

Utsu, T., 1970. Aftershocks and earthquake statistics, *J. Faculty Sci. Hokkaido Univ. Japan, Ser. VII.,* **3**(Part II), 197–266.

Utsu, T., 1971. Aftershocks and earthquake statistics, *J. Faculty Sci. Hokkaido Univ. Japan, Ser. VII,* **3**(Part III), 379–441.

Wessel, P. & Smith, W.H.F., 1991. Free software helps map and display data, *Eos Trans., AGU,* **72,** 441.

Wiemer, S. & Katsumata, K., 1999. Spatial variability of seismicity parameters in aftershock zones, *J. geophys. Res.,* **103,** 13 135–13 151.

Wiemer, S. & Wyss, M., 1997. Mapping the frequency-magnitude distribution in asperities: an improved technique to calculate recurrence times?, *J. geophys. Res.,* **102,** 15 115–15 128.

Wiemer, S. & Wyss, M., 2000. Minimum magnitude of completeness in earthquake catalogs: examples from Alaska, the western United States and Japan, *Bull. seism. Soc. Am.,* **90**(4), 859–869.

Woessner, J. & Wiemer, S., 2005. Assessing the quality of earthquake catalogs: estimating the magnitude of completeness and its uncertainty*, Bull. seism. Soc. Am.,* **95,** 684–698.

Wyss, M., 1973. Towards a physical understanding of the earthquake frequency distribution, *Geophys. J. R. astr. Soc.,* **31,** 341–359.

Wyss, M., 1997. Second round of evaluations of proposed earthquake precursors, *Pure appl. Geophys.,* **149,** 3–16.

Wyss, M. & Booth, D.C., 1997. The IASPEI procedure for the evaluation of earthquake precursors, *Geophys. J. Int.,* **131**(3), 423–424.

Wyss, M. & Lee, W. H. K, 1973. Time variation of the average earthquake magnitude in Central California, in *Proceedings of the Conf. Tectonic Problems of the San Andreas Fault System,Geol. Sci.,* vol. 13, eds Kocach, and Nur, pp. 24–42, Stanford, Calif.: Stanford Univ.

Zaliapin, I. & Ben-Zion, Y., 2015. Artefacts of earthquake location errors and short-term incompleteness on seismicity clusters in southern California, *Geophys. J. Int.,* **202**(3), 1949–1968.

Zúñiga, F.R. & Wyss, M., 1995. Inadvertent changes in magnitude reported in earthquake catalogs: their evaluation through b-value estimates. *Bull. Seism. Soc. Am,* **85**(6), 1858–1866.

SUPPORTING INFORMATION

Supplementary data are available at *GJI* online.

Figure S1. Uncertainty of b_{est} for 10^5 simulated samples, as function of sample size N, of magnitude range ΔM and of true *b*-value b. The relation between $\Delta b = b_{est}/b$ and $\Delta M{\cdot}b$ is independent of b. The uncertainty of b_{est} decreases with the increase of N and ΔM. The sold lines mark the median value, for each N and ΔM. The small panel shows a zoom for smaller ranges of Δb and ΔM.

Figure S2. Estimation of M_c and b_{ref} for events occurred in the ER before (grey points) and after (black points) the 2012 sequence. The solid lines mark the estimated GR law.

Figure S3. The same as Fig. 3 but for $N_{tw} = 250$.

Figure S4. Estimation of b_{est} for events occurred in the CIR, during the periods $P1$, $P2$ and $P3$, excluding the 2009 L'Aquila and 2016 CI sequences, for a) $N_{tw} = 500$ and b) $N_{tw} = 1000$. The dotted red lines mark the median values, giving the reference *b*-value b_{ref} of the region.

Figure S5. The same as Fig. 4 but for $N_{tw} = 250$.

Figure S6. The same as Fig. 5 but for $N_{tw} = 250$.

Figure S7. Plot of magnitudes of the immediate aftershocks versus the logarithmic time after the main shock, for the three (a) 2012 Emilia, (b) 2009 L'Aquila and (c) 2016–2017 Central Italy sequences.

Movie S1. Movie with all M_c and *b*-value maps for the Emilia region ($N_{tw} = 500$, $R = 10$).

Movie S2. Movie with all M_c and *b*-value maps for the Central Italy region ($N_{tw} = 500$, $R = 10$), from 2005 April 16 to 2016 October 30.

Movie S3. Movie with all M_c and *b*-value maps for the Central Italy region ($N_{tw} = 500$, $R = 10$), from 2016 October 30 to 2021 April 30.

Please note: Oxford University Press is not responsible for the content or functionality of any supporting materials supplied by the authors. Any queries (other than missing material) should be directed to the corresponding author for the paper.